PRELIMINARY STUDY OF A RADIO FREQUENCY INTERFERENCE FILTER FOR NON-POLARIMETRIC C-BAND WEATHER RADAR IN INDONESIA (CASE STUDY: TANGERANG WEATHER RADAR)

Abdullah Ali[1], Iddam Hairuly Umam[1], Hidde Leijnse[2], Umi Sa'adah[3]
[1]Remote Sensing Data Management Division, Center for Public Weather Service, Indonesia Agency for Meteorology Climatology and Geophysics (BMKG)
[2]The Royal Netherlands Meteorological Institute (KNMI)
[3]Jakarta Meteorological Watch Office BMKG Soekarno-Hatta
*e-mail: abdullah.ali@bmkg.go.id
Received: 27 December 2020; Revised: 31 December 2021; Approved: 24 January 2022

Abstract. C-Band weather radar that operates at a frequency of 5 GHz is very vulnerable to radio frequency interference (RFI) because it is located on a free used frequency. RFI can cause image misinterpretation and precipitation echo distortion. The new allocation for free spectrum recommended by the World Radio Conference 2003 and weather radar frequency protection in Indonesia controlled by the Balai Monitoring Spektrum Frekuensi (BALMON) have not provided permanent protection against weather radar RFI. Several RFI filter methods have been developed for polarimetric radars, but there have been no studies related to RFI filters on non-polarimetric radars in Indonesia. This research aims to conduct an initial study of RFI filters on such radars. Four methods were applied in the initial study. The Himawari 8 cloud mask was used to eliminate interference echo based on VS, IR, and I2 channels, while the nature of false echo interference that does not have a radial velocity value was used as the basis for the application of the Doppler velocity filter. Another characteristic in the form of consistent echo interference up to the maximum range was used as the basis for applying a beam filling analysis filter with reflectivity thresholds of 5 dBZ and 10 dBZ, with beam filling of more than 75%. Finally, supervised learning Random Forest (RF) was also used to identify interference echo based on the characteristics of the sampling results on reflectivity, radial velocity, and spectral width data. The results show that the beam filling analysis method with a threshold of 5 dBZ provides the best RFI filter without eliminating echo precipitation.

Keywords: *weather radar, radio frequency interference, filtering algorithm*

1 INTRODUCTION

The radio wave spectrum is a global resource that is used in many sectors, such as telecommunications, remote sensing, and navigation, amongst others, either by the public or the military (Cho, 2017). The use of wireless internet devices operating at a frequency of 5 GHz is claimed to influence C-Band weather radar observations in the form of radio wave interference (Saltikof, 2016; Joe et al., 2005). At the World Radio Conference 2003 (WRC-2003), there was a recommendation for a new allocation of free frequencies in the 5470 – 5725 MHz spectrum as some essential operational systems such as weather and military radar have the potential for interference (ITU-R 229, 2003). Interference is a superposition of two electromagnetic waves at the same frequency or adjacent ones, producing a new wave pattern (Wardoyo, 2014). This interference can cause inaccuracies in weather radar

http://dx.doi.org/10.30536/j.ijreses.2021.v18.a3727

observations and image misinterpretation. One of the most significant impacts of this is overestimation in quantitative precipitation estimation (QPE) products (Ali, 2020).

Until 2021, BMKG had operated 38 C-Band weather radars to support meteorological operational activities in providing weather information and early warnings, ranging from public and aviation to maritime weather information (Ali, 2021 SIDARMA). Not only used in meteorological operations, BMKG weather radar data installed in Tangerang has also been used as input for flood forecasting models in Jakarta in the Jakarta-Flood Early Warning Systems (J-FEWS) system (Ginting, 2014). This makes the filtering process for non-meteorological echoes an essential priority.

There are several non-meteorological echo sources that have the potential to occur in Indonesia. Its highly variable topography and urban environment can cause the radar to detect ground clutter and beam blocking (McRoberts & Nielsen-Gammon, 2017). In addition, sea clutter is often detected on radars installed on small islands or near the sea (Hailong et al., 2019). Radio frequency interference commonly occurs on the C-Band weather radar that operates at a frequency of 5600-5650 MHz, which is included in the free frequency allocation (Wardoyo, 2014). Radio frequency interference often occurs on weather radars installed in dense urban areas due to the widespread use of wireless internet devices. The results of the BMKG weather radar observations show that the Tangerang weather radar experiences the most severe interference.

Radio wave interference that occurs on weather radar can produce a significant false echo with a spike-shaped characteristic. This can lead to the perception of precipitation in fair weather (Keränen et al., 2013). When bad weather occurs, interference causes superimposed with precipitation echo, resulting in distortions in measurement and identification (Yin et al., 2021). Interference that occurs continuously will cause overestimated results for QPE products, where false echoes due to interference will appear as very high rainfall intensity (Ali, 2020).

Several mitigation efforts have been made to minimise the potential for weather radar interference. The International Telecommunications Union (ITU) has set a standard Dynamic Frequency Selection (DFS) algorithm, but it is not able to provide permanent protection against potential weather radar interference (Wardoyo, 2014). The Frequency Spectrum Monitoring Centre (BALMON) has also made protection efforts by conducting sweeping based on reports of interference disturbances by the BMKG (Firdaus & Suryadi, 2019). These efforts often encounter problems when the source of interference already exists before the weather radar is installed. The final step is to filter the data from weather radar observations.

Several radio frequency interference (RFI) filter algorithms have been investigated. The two-dimensional (2D) range-time/sample-time domain RFI filter algorithm functions by analysing the amplitude-anomaly-based RFI (Cho, 2017). The spectral filter algorithm applied to polarimetric radar suppresses RFI by analysing the Doppler power spectrum time series data in each polarisation to obtain interference characteristics (Rojas, 2012). However, there has been no research on the use of non-polarimetric radar observation data as an RFI filter. This paper aims to test RFI filtering using the results of non-polarimetric weather radar observations (reflectivity, radial velocity, and spectral

width) combined with the results of weather satellite observations.

2 MATERIALS AND METHODOLOGY

2.1 Tangerang Weather Radar

The study used non-polarimetric C-Band weather radar with a 200 km maximum range, 250 m spatial resolution, and nine elevation angles. Figures 2-1 and 2-2 show the radar scanning strategy and beam blockage analysis. The scanning strategy was optimised to enable dense observation at a low elevation to maximise precipitation detection. There is significant terrain blocking at the elevation of 0.5° due to mountain ranges and several hills to the south of the radar, but at the elevation of 1.5° the blocking is not significant. The radar hardware specification and scanning strategy is shown at Table 2-1.

2.2 Study area

The study area covered 220 km around the Tangerang weather radar point location, including both land and the part of the Java Sea. The historical observations of the radar show that RFI most often occurs at the two lowest elevations (0.5° and 1.5°). The data used for the RFI filtering trial were Tangerang weather radar data from September 9, 2018 and May 5, 2021. Four methods were used in the RFI filter: the Himawari-8 cloud mask, beam filling analysis, the Doppler filter, and supervised machine learning Random Forest (RF).

2.3 Methods

Interference false echo comes from non-meteorological object sources, so in theory Himawari-8's cloud masking overlay can filter meteorological objects from interference sources that are not meteorological. The channels used for the cloud mask were Band 03 (VS), Band 13 (IR) and Band 15 (I2), with the threshold for the non-cloud category being IR over 265 K; the difference between IR and I2 greater than 2 K; and reflectance VS less than 0.45. The results of the cloud masking product were then resampled against the resolution of the weather radar data, and then these data at the non-cloud grid location were eliminated as an interference filter.

Table 2-1: Tangerang weather radar specification and scanning strategy

Parameter	Value
Radar site name	Tangerang
Polarisation	Single
Installation year	2009
Manufacturer	EEC
Signal Processor	GDRX-SP
Transmitter Type	Coaxial magnetron
Latitude	-6.1669° S
Longitude	106.6502° E
Altitude	10 m
Tower height	20 m
Frequency	5.6 GHz
Beam width	1°
Pulse width range	0.5 - 2.0 µs
Pulse width used	0.8 µs
PRF Used	600 Hz
Staggering	¾
Range step	250 m
Range maximum	220 km
Number of sweeps	9
Nyquist Velocity	24.1 m/s
VCP Mode	Free run (8 minutes interval)
Moment observed	Reflectivity (unfiltered and filtered), radial velocity, spectral width

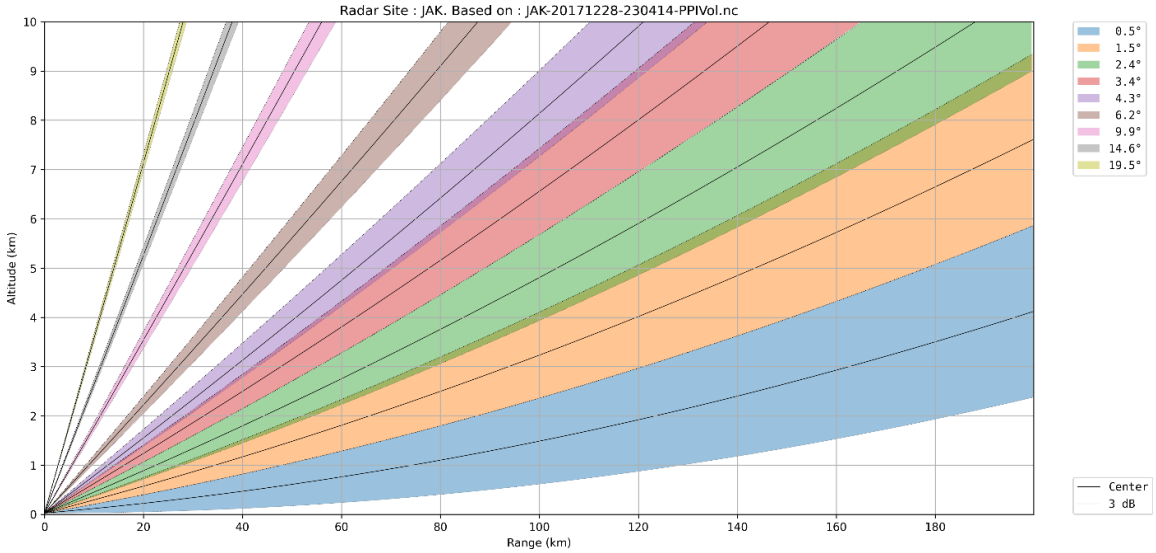

Figure 2-1: Tangerang weather radar scanning strategy

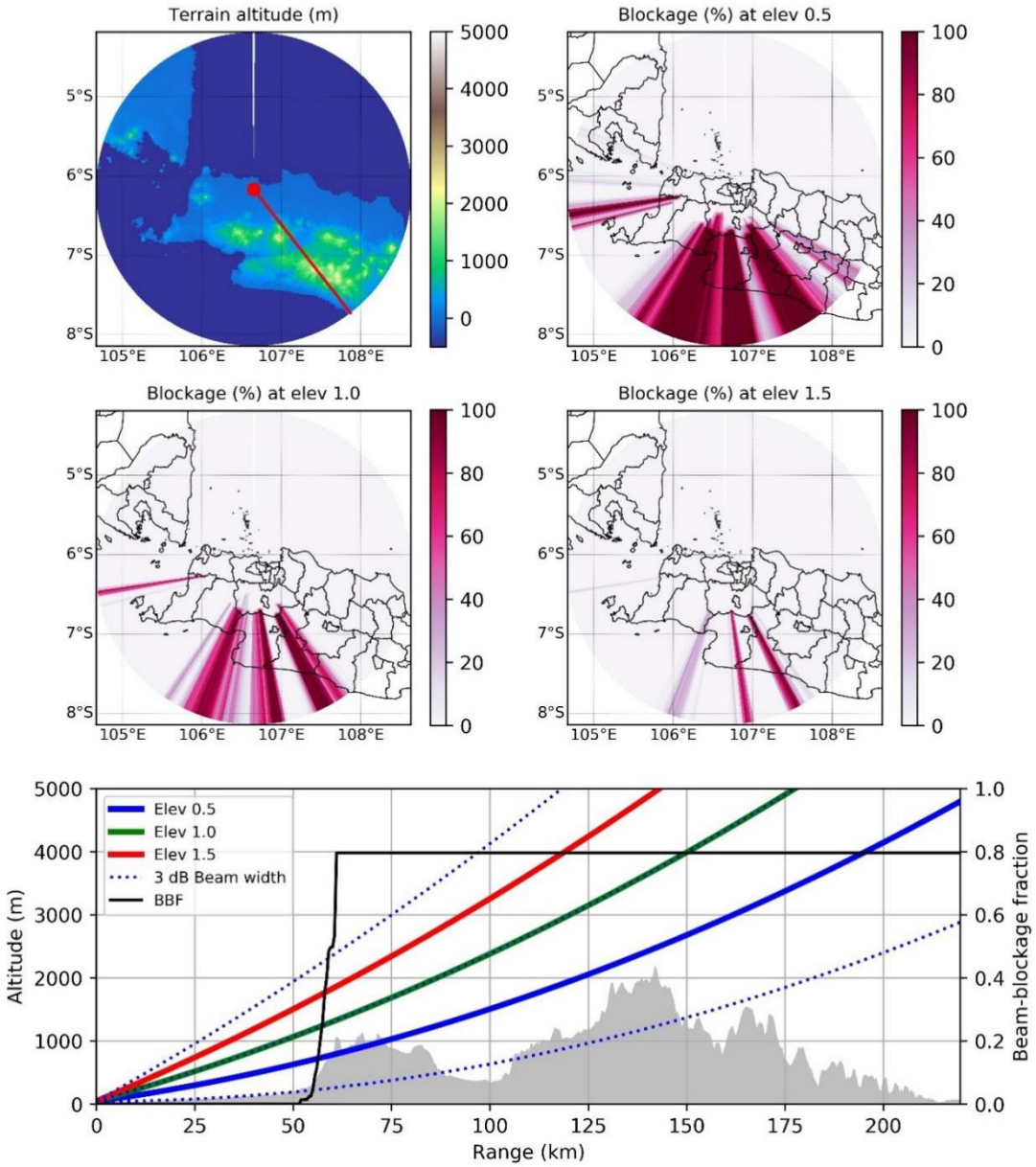

Figure 2-2: Tangerang weather radar beam blockage analysis.

Non-meteorological echoes sometimes have radial velocity values, such as echoes from volcanic ash, sea clusters, or ground clutter echoes from animals (Hubbert et al., 2009). The value of radial velocity is calculated based on the movement of objects in the radial direction (towards or away from) the weather radar (Doviak et al., 1979). False echo interference comes from sources of radio wave transmitters with the same/close frequency, so there is no movement at the interference source, with the implication that the radial velocity value is not detected. This concept is used for RFI filtering, in which the radial velocity value is nan (not a number). The value of nan is different from the value of 0 in the radial velocity, because when the object moves perpendicularly to the direction of the radar sweep, the value of the radial velocity is 0, a pattern which is called a zero isodop, while for objects that are not moving, the value of the radial velocity will be nan. The radial velocity value is extracted at each azimuth. This method will hereinafter be referred to as the Doppler Velocity Filter.

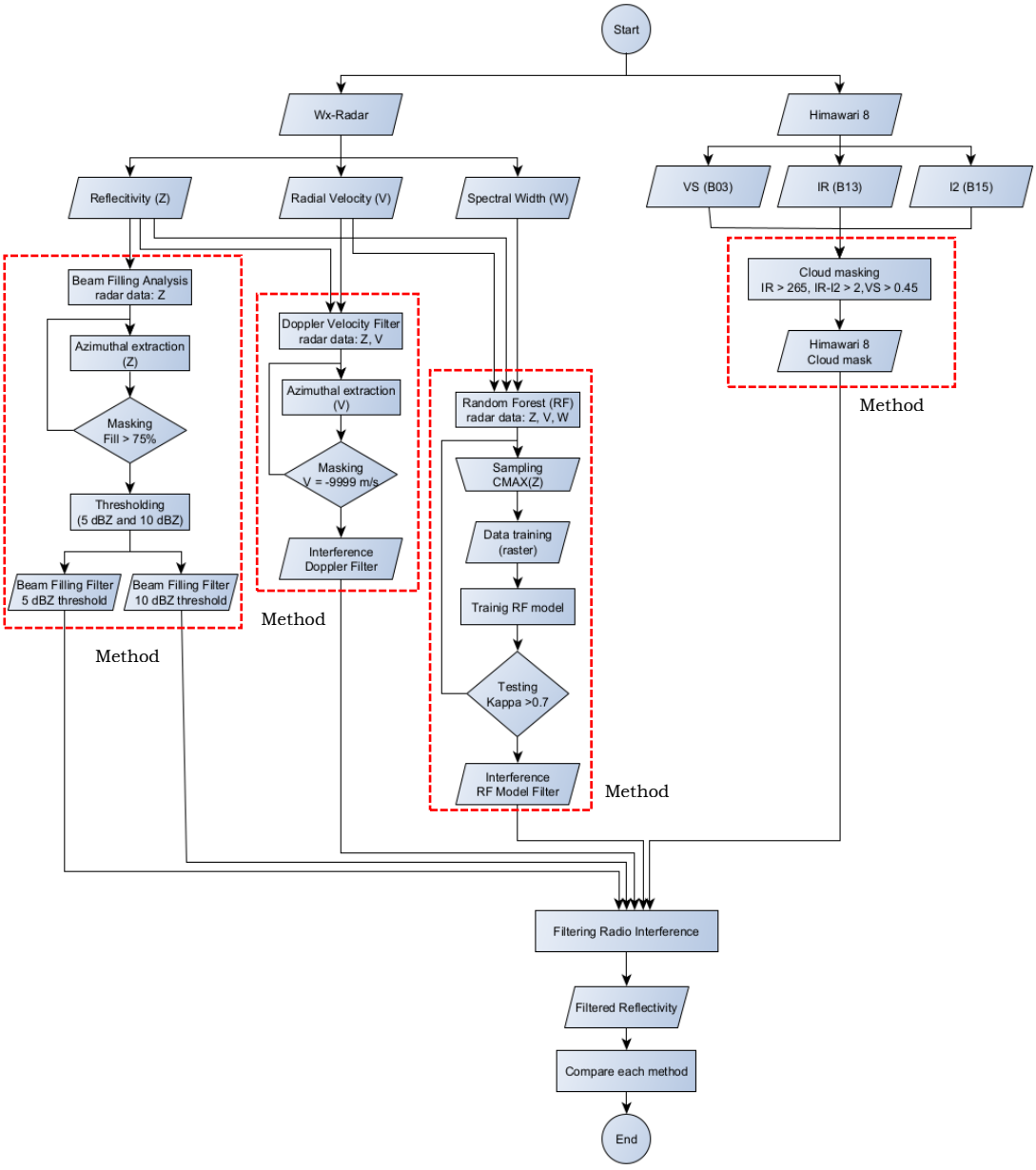

Figure 2-3: Research flowchart

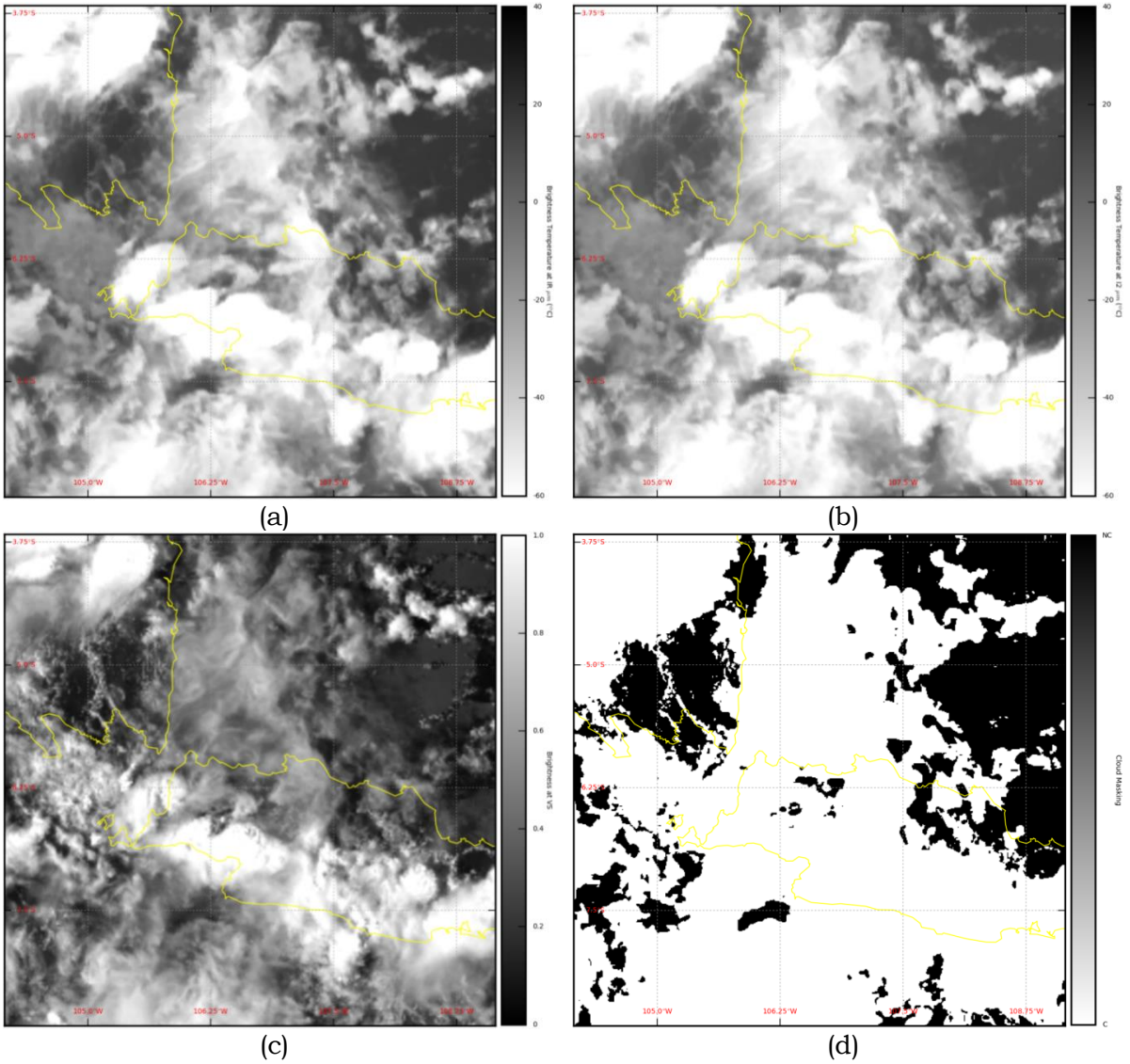

Figure 3-1: Himawari-8 cloud mask and results of the RFI filter: (a) IR, (b) I2, (c) VS, (d) Cloud mask. Unfiltered reflectivity (f) Filtered reflectivity using Himawari-8 cloud mask

False echo interference has a spike pattern that reaches a maximum radius. This has implications for the percentage of beam filling at each azimuth. The consistency of beam filling from the source of interference to the maximum radius of the reflectivity data is one of the characteristics of RFI. This concept was later developed into an RFI filtering method, in which an azimuth that has a beam filling of more than 70% of the maximum radius, and exceeds the specified reflectivity threshold, is considered to be a false echo, and is deleted. In this initial study, two thresholds were used which were considered as false echo interference, namely 5 dBZ and 10 dBZ. The method is hereinafter referred to as beam filling analysis. In this method, only reflectivity data are used for filtering, in contrast to the Doppler velocity filter, which uses reflectivity and radial velocity data.

The next method was supervised machine learning Random Forest (RF). This is very popular in the identification algorithm where the data classification sample has been determined (Breiman, 2001; Pal, 2005). The sampling process was conducted on three types of data (reflectivity, radial velocity, and spectral width) to obtain two classifications, namely meteorological echo, and interference echo. Before the model was

run for RFI filtering, testing is conducted to test the model's accuracy performance based on the kappa value. When this value is greater than 0.7, the model can continue to the echo interference elimination process. If the value is lower than 0.7, the number of samples is increased.

To facilitate the naming identification of the methods to be employed, they were renamed. The Himawari-8 cloud mask filter is hereinafter referred to as method 1, the Doppler velocity filter method 2, the beam filling analysis filter method 3, and the RF filter is called method 4. The flow of data processing in these four methods is shown in Figure 2-3. The RFI filter results from the four models were then compared based on the resulting filtered reflectivity.

3 RESULTS AND DISCUSSION

The Tangerang weather radar imagery of November 9, 2018 at 07.50 UTC experienced interference in almost all directions. As shown in Figure 3-1, interference occurred from the north to the southeast, where there is no meteorological echo. This can lead to the misinterpretation of "precipitation in fair weather". In addition, interference in the south to west direction causes the echo precipitation to be distorted by the interference echo, leading to interference with image interpretation.

The results of the Himawari-8 weather satellite data processing IR, I2, and VS channels to create cloud mask products, along with a comparison of th filter results, are shown in Figure 3-2. The difference in spatial resolution (Himawari-8 1km, weather radar 250m) was overcome by resampling the satellite data to adjust the resolution of the weather radar data. The satellite data used were adjusted to the radar observation time.

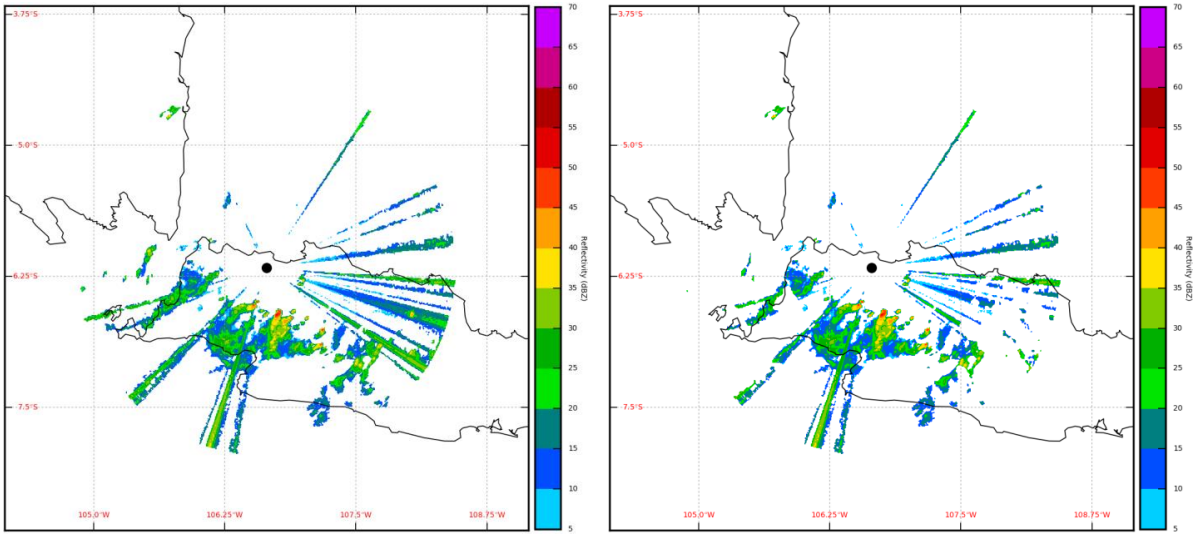

Figure 3-2: Himawari-8 cloud mask and RFI filter results. (a) IR, (b) I2, (c) VS, (d) Cloud mask. Unfiltered reflectivity (f) Filtered reflectivity using Himawari-8 cloud mask

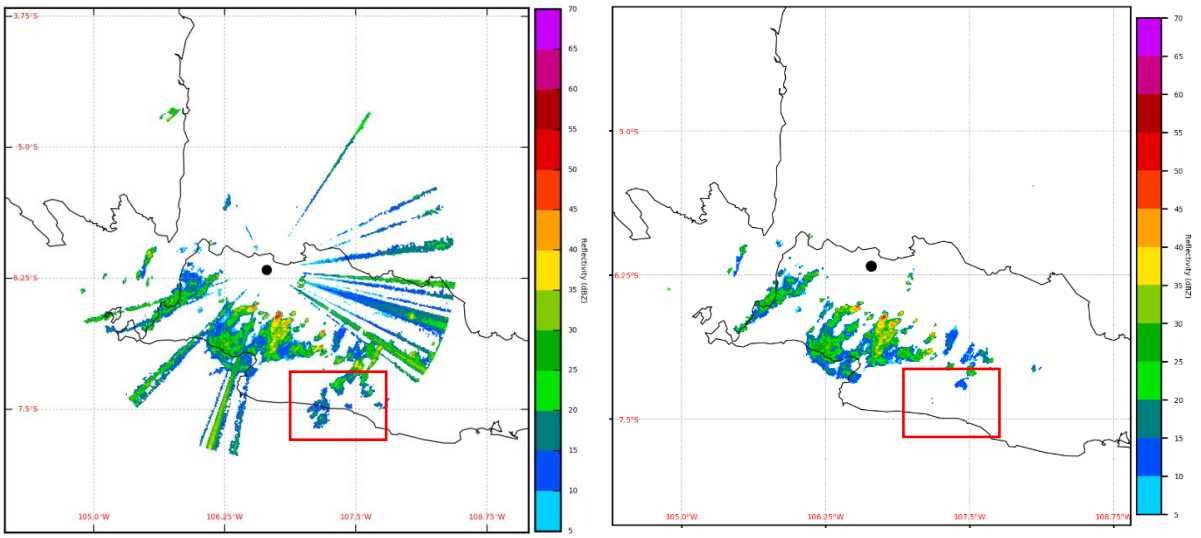

Figure 3-3: Doppler velocity filter results from eliminating false echoes from RFI. The false echo is eliminated, but some precipitation echo is accidentally removed. This can be happen when the SQI value is low. (a) Unfiltered maximum reflectivity, (b) RFI filtered maximum reflectivity.

The Himawari-8 cloud mask results show that almost all the pixels are clouds. This has implications for RFI filtering, where only a small portion of false echo interference is eliminated by the RFI cloud mask filter. There are several reasons why the cloud mask does not completely eliminate echo interference. The relatively large difference in spatial resolution and the orientation of the different cloud observations are the two most powerful causal factors. Weather radar observes clouds by actively emitting radio waves from below them, while the Himawari-8 satellite passively observes them from above by receiving radiation generated by the clouds.

The Doppler velocity filter method was applied to the two lowest elevations of the Tangerang weather radar. The no data value of the Tangerang weather radar radial velocity data was expressed with a value of -3269, so the value of the radial velocity extraction results at each azimuth of the two lowest elevations was used as an RFI filter. Elimination of echo interference was not made at maximum reflectivity, but only at the lowest two elevations, with data from other elevations then applied in the CMAX (Column Maximum) algorithm. The results of the elimination of echo interference using the Doppler velocity method are shown in Figure 3-3. This method produces an image that is free of echo interference, but there are some missing echo precipitations (region in the red square). This is quite surprising as echo precipitation can be worth as no data at radial velocity. This is likely to occur in precipitation echoes with low reflectivity values and low signal quality index (SQI) values, so the radar will consider the radial velocity value as no data when the SQI value is low.

The basic concept of using beam filling analysis for RFI filters is the general characteristic of echo interference, which has a consistent spike pattern until it reaches the bin in the maximum range. Thresholds of 5 dBZ and 10 dBZ are used because there is variability in the reflectivity data extraction results at each azimuth, where at a certain time the minimum reflectivity value can reach 5 dBZ or 10 dBZ.

Based on Figure 3-2(a), the wrong azimuth value affected by RFI is at 98.8°.

The results of beam filling analysis at 98.8° azimuth and the reflectivity values (dBZ) and received power (dB) are shown in Figure 3-4. The beam filling graph clearly shows the difference between echo precipitation and echo interference, where echo precipitation is characterised by "natural variability", while echo precipitation consistently has a high percentage of beam filling; therefore, the threshold of 75% is taken as an initial study. The reflectivity profile of the interference echo tends to increase along with the increase in the bin range, but when returned to the power received value, the interference echo has the same power.

The results of the beam filling analysis filter with thresholds of 5 dBZ and 10 dBZ are shown in Figure 3-5. When compared with the unfiltered maximum reflectivity, the interference echo is mostly eliminated without any loss of precipitation echo, in contrast to the Doppler velocity filter method which can eliminate all interference echoes, but there are some precipitation echoes that are removed. Some interference echoes remain at the thresholds of 5 dBZ and 10 dBZ. This shows that there are several interference echoes with weak intensity that are not consistently present up to the maximum bin range.

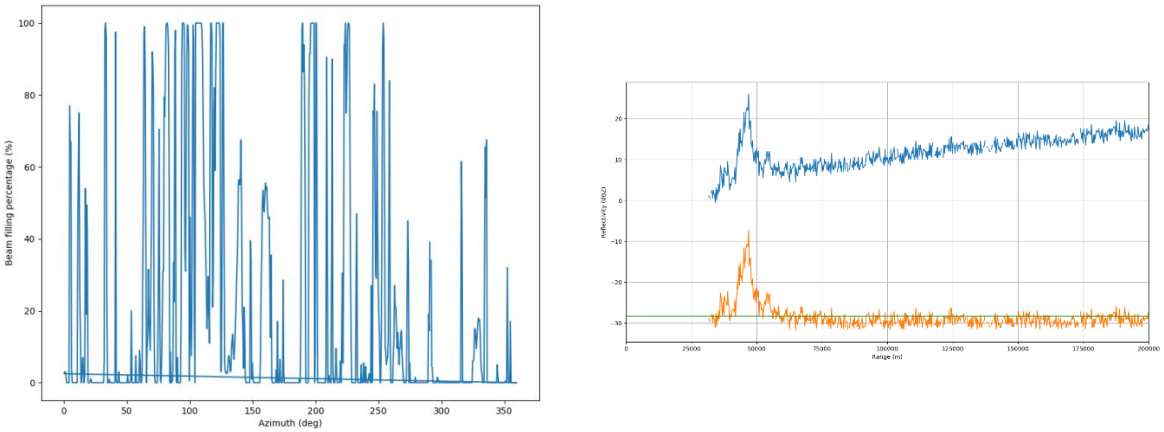

Figure 3-4: Beam filling percentage, reflectivity, and received power profile at azimuth 98.8°.

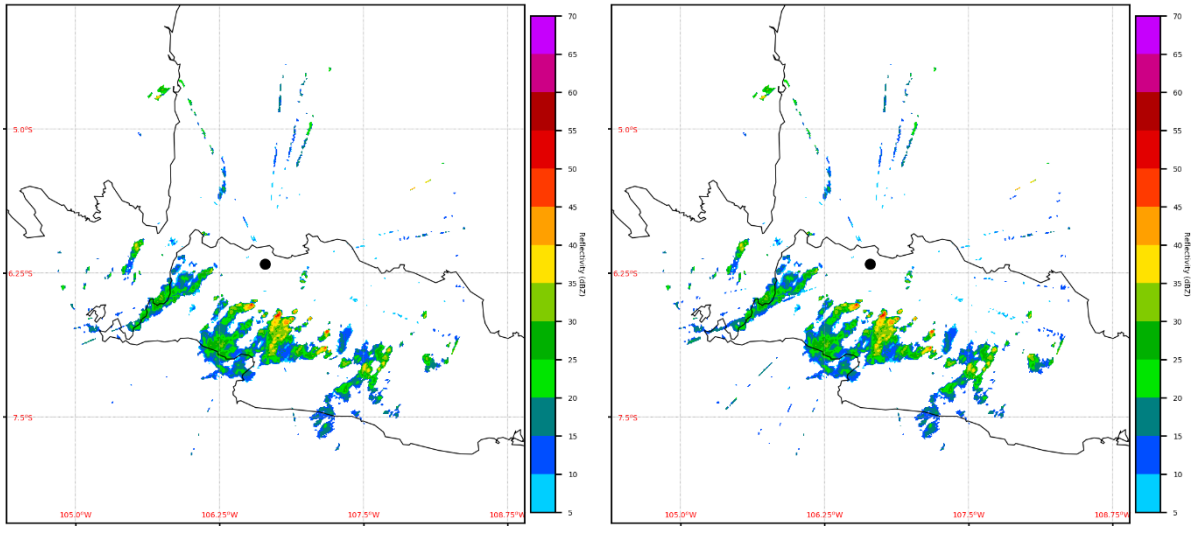

(a) (b)

Figure 3-5: RFI filter for 75% percentage of beam filling. (a) 5 dBZ threshold, (b)10 dBZ threshold

The 5 dBZ threshold provides a relatively better filter than the 10 dBZ one, especially in the southwest part of the weather radar, while in the other direction the results are the same as the 10 dBZ threshold. Further research is needed on the minimum threshold value for echo interference. When compared to the results of the Doppler velocity filter, which can eliminate all echo interference, the beam filling analysis filter method can be elevated by adding a Doppler velocity filter step. It is certain that the remnants of echo interference that cannot be filtered out by this method do not have a radial velocity value, so the selection process for echo interference through the percentage of beam filling can be continued with selection based on the radial velocity value. The beam filling analysis method has drawbacks if the precipitation system that occurs is meso-scale and reaches more than the beam filling percentage threshold. Under these conditions, the precipitation echo will be considered as interference echo and will be eliminated.

It is possible to classify echo interference using machine learning-based methods. One of the most popular methods used in remote sensing to classify images is Random Forest. The model development process is conducted through manual sampling as the sampling process emphasises the interference echo pattern, which is quite difficult to detect by the machine without supervision. The classification of data determined in the sampling process is divided into three classes, precipitation echo, interference echo, and clear/no echo. Initial sampling was made on the maximum reflectivity data, then the location of the point/polygon was also applied to the radial velocity and spectral width data at the lowest elevation (0.5%). The results of the sampling on reflectivity, radial velocity, and spectral width data were then used to build a classification model.

Unfiltered reflectivity, sampling, and the results of the classification model of the supervised RF method are shown in Figure 3-6. The kappa value of the model testing results is 0.9, meaning the RF model can continue to the classification process. The results of the classification of the echo interference from the RF model show interference with weak intensity in the southeast and northwest directions. There is a misclassification of the superimposed interference echo with the precipitation echo, especially in the northeast and southwest directions. Convective systems that have low reflectivity values at the edges are considered as interference echoes because of similar reflectivity data values, but interference echoes that are not superimposed with precipitation echoes can be detected properly.

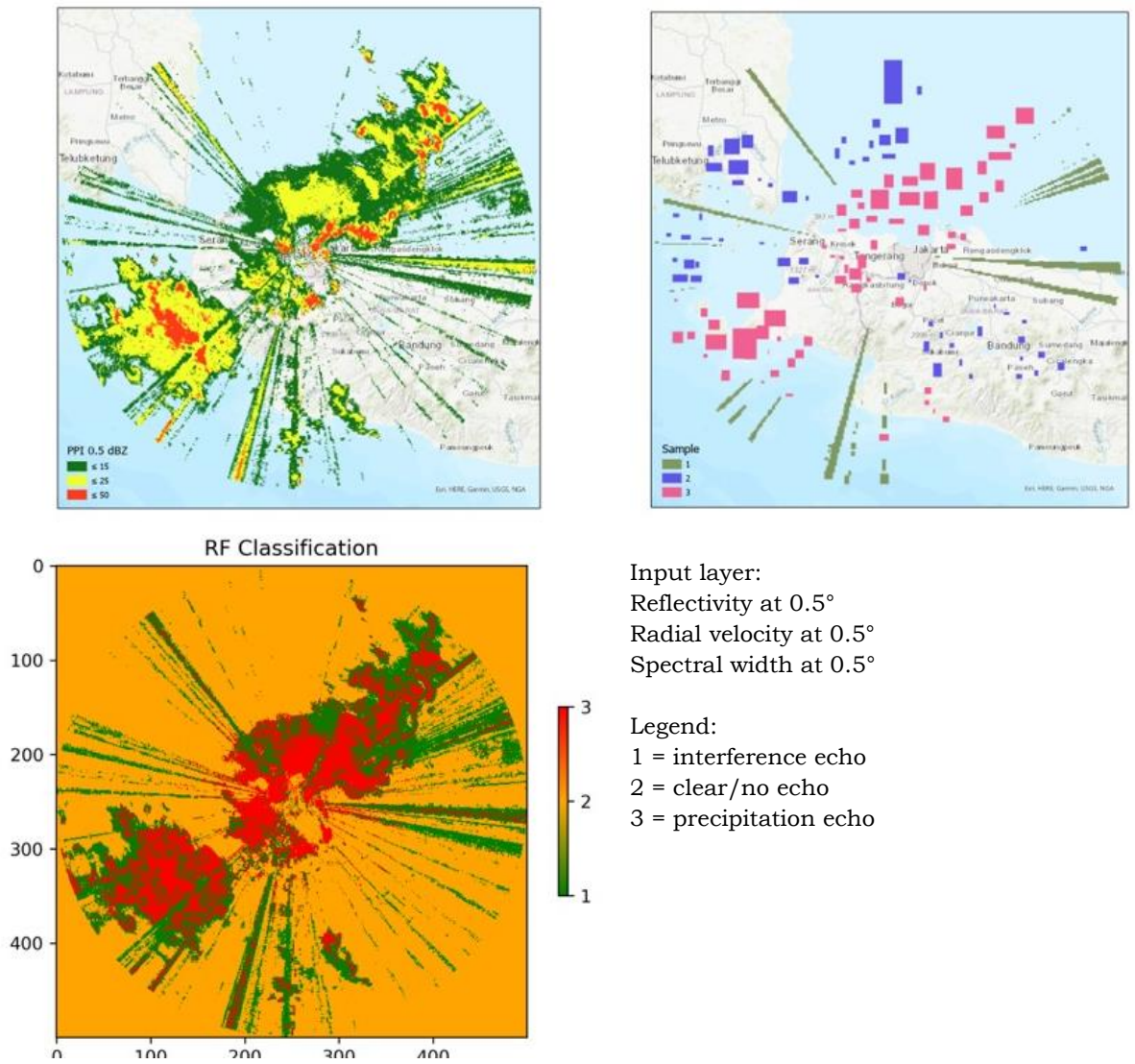

Figure 3-4: RF classification

4 CONCLUSIONS

The initial study of the RFI filter on the Tangerang weather radar applied four methods based on data from weather radar observations and Himawari-8 weather satellite data. The first method used the Himawari-8 cloud mask product to eliminate echo interference by eliminating echo at no cloud grid locations. The second method employed radial velocity data with the basic concept that echo interference has no radial velocity value because it is not a meteorological object. The characteristics of echo interference with consistent beam filling consistency up to the maximum range were used as the basis for the beam filling analysis filter method, in which the results of the extraction of reflectivity values for each azimuth that have a beam filling percentage of more than 75% are considered to be interference echoes. In the initial study, two threshold reflectivity values were determined, namely 5 dBZ and 10 dBZ. The fourth method was image classification based on supervised machine learning Random Forest.

Based on historical data, RFI on the Tangerang weather radar most often occurs at the last two elevations, so the RFI filter was only employed on these. Himawari-8's cloud mask product is only able to partially eliminate echo interference; this can be due to

differences in spatial resolution and in observation techniques between radar and weather satellites. The Doppler velocity filter method can eliminate all interference echoes, but some of the precipitation echoes are also eliminated. This may be due to the low SQI value, meaning that the radial velocity value is considered as no data. The performance of the beam filling analysis method is relatively good, especially at the 5 dBZ threshold, but there are still some weak interference echoes that are not filtered because the reflectivity value is less than the threshold used. The RF model gives fairly accurate results in classifying the interference echo, but there is a misclassification of the superimposed interference echo with the precipitation echo.

There are several weaknesses evident in each method. Among the four, the best performance was from the beam filling analysis filter with thresholds, while the worst was the Himawari-8 cloud mask filter. The beam filling analysis method has a weakness in the threshold used, which in each case can be different. This method can be elevated in combination with a Doppler velocity filter, where weak unfiltered interference can be eliminated because it can be ascertained that it does not have a radial velocity value. The weakness of the RF model in classifying interference echoes lies in the limited input of non-polarimetric radar training data, which only produces three types of data (reflectivity, radial velocity, and spectral width), so that when echo interference occurs in precipitation echoes, the reflectivity values will be considered as echo interference.

ACKNOWLEDGEMENTS

The research data were fully supported by BMKG Weather Radar Data Management Subdivision. The paper was improved by the helpful suggestions of Dr. Hidde Leijnse from KNMI Netherlands. The author wishes to thank all those who helped in the research.

AUTHOR CONTRIBUTIONS

Lead author: Abdullah Ali. Co-Author: Iddam Hairully Ummam, Hidde Ljeinse, Umi Sa'adah.

Author contributions are as follows: Abdullah Ali: Weather radar processing, RFI filter, results analysis. Iddam Hairuly Umam: Provision of introduction, map layouting, prepare draft manuscript. Hidde Ljeinse: conceptualization and methodology. Umi Sa'adah: Provision of Tangerang weather radar data.

REFERENCES

Ali, A., Adrianto, R., & Saepudin, M. (2019). Preliminary Study Of Horizontal And Vertical Wind Profile Of Quasi-Linear Convective Utilizing Weather Radar Over Western Java Region, Indonesia. International *Journal of Remote Sensing and Earth Sciences (IJReSES), 15*(2), 177-186.

Ali, A., Deranadyan, G., & Umam, I. H. (2020). An Enhancement to The Quantitative Precipitation Estimation Using Radar-Gauge Merging. *International Journal of Remote Sensing and Earth Sciences (IJReSES), 17*(1), 65-74.

Ali, A., Supriatna, S., & Sa'adah, U. (2021). Radar-Based Stochastic Precipitation Nowcasting Using The Short-Term Ensemble Prediction System (Steps)(Case Study: Pangkalan Bun Weather Radar). *International Journal of Remote Sensing and Earth Sciences (IJReSES), 18*(1), 91-102.

Breiman, L. (2001). Random forests. *Machine Learning, 45*(1), 5-32.

Cho, J. Y. (2017). A new radio frequency interference filter for weather radars. Journal of Atmospheric and Oceanic *Technology*, 34(7), 1393-1406.

Doviak, R. J., Zrnic, D. S., & Sirmans, D. S. (1979). Doppler weather radar. *Proceedings of the IEEE, 67*(11), 1522-1553.

Firdaus, T., & Suryadi, D. (2019). Analisis Interferensi Frekuensi Radio Radar Cuaca Badan Meteorologi Klimatologi Dan Geofisika (BMKG) Di Kalimantan Barat. *Jurnal Teknik Elektro Universitas Tanjungpura, 2*(1).

Ginting, S. (2014). Sistem peringatan dini banjir Jakarta. *Jurnal Sumber Daya Air, 10*(1), 71-84.

Hailong, W., Shouyuan, D., Xu, W., & Zhao, S. (2019, December). Sea clutter recognition based on dual-polarization weather radar. *In 2019 International Conference on Meteorology Observations (ICMO)* (pp. 1-3). IEEE.

Hubbert, J. C., Dixon, M., Ellis, S. M., & Meymaris, G. (2009). Weather radar ground clutter. Part I: Identification, modeling, and simulation. *Journal of Atmospheric and Oceanic Technology, 26*(7), 1165-1180.

ITU-R Radio Communication Study Groups, documents 8A/103-E and 8B/65-E, August 30, 2004. *Studies on the effect of wireless access systems including RLANs on terrestrial meteorological radars operating in the band 5600-5650 MHz.* International Telecommunication Union (ITU), Geneva, Switzerland.

Joe, P., Scott, J., Sydor, J., Brandão, A., & Yongacoglu, A. (2005, October). Radio local area network (RLAN) and C-band weather radar interference studies. *In Proc. 32nd AMS Radar Conference on Radar Meteorology*.

Keränen, R. E. I. N. O., Rojas, L., & Nyberg, P. E. T. R. I. (2013). Progress in mitigation of WLAN interferences at weather radar. *In 36th Conf. on Radar Meteorology*.

McRoberts, D. B., & Nielsen-Gammon, J. W. (2017). Detecting beam blockage in radar-based precipitation estimates. *Journal of Atmospheric and Oceanic Technology, 34*(7), 1407-1422.

Moon, J., & Ryu, C. (2017). WiFi (RLAN) and a C-Band Weather Radar Interference. *Journal of the Chosun Natural Science, 10*(4), 216-224.

Pal, M. (2005). Random forest classifier for remote sensing classification. *International Journal of Remote Sensing, 26*(1), 217-222.

Rojas, L., Moisseev, D. N., Chandrasekar, V., Selzler, J., & Keränen, R. (2012). Dual-polarization spectral filter for radio frequency interference suppression. *In Preprints, Seventh European Conf. on Radar in Meteorology and Hydrology (ERAD 2012), Toulouse, France*. Météo-France.

Saltikoff, E., Cho, J. Y., Tristant, P., Huuskonen, A., Allmon, L., Cook, R., Becker, E., & Joe, P. (2016). The threat to weather radars by wireless technology. *Bulletin of the American Meteorological Society, 97*(7), 1159-1167.

Wardoyo, E. (2014). Analisis Interferensi Frekuensi Radar Cuaca C-Band di Indonesia. *InComTech: Jurnal Telekomunikasi dan Komputer, 5*(2), 163-184.

Yin, J., Chen, H., Li, Y., & Wang, X. (2021). Clutter Mitigation based on Spectral DepolarizationRatio for Dual-polarization Weather Radars. *IEEE Journal of Selected Topics in Applied Earth Observations and Remote Sensing.*